

Document downloaded from:

<http://hdl.handle.net/10251/158496>

This paper must be cited as:

Gómez Pinedo, U.; Sanchez-Rojas, L.; Vidueira, S.; Sancho, FJ.; Martínez-Ramos, C.; Lebourg, M.; Monleón Pradas, M.... (2019). Bridges of biomaterials promote nigrostriatal pathway regeneration. *Journal of Biomedical Materials Research Part B Applied Biomaterials*. 107(1):190-196. <https://doi.org/10.1002/jbm.b.34110>



The final publication is available at

<https://doi.org/10.1002/jbm.b.34110>

Copyright John Wiley & Sons

Additional Information

Bridges of biomaterials promote nigrostriatal pathway regeneration

Ulises Gómez-Pinedo ^{1,2*} Leyre Sanchez-Rojas,^{2*} Sandra Vidueira,¹ Francisco J. Sancho,¹ Cristina Martínez-Ramos,^{1,3,4} Myriam Lebourg,^{3,4} Manuel Monleón Pradas,^{1,3,4} Juan A. Barcia^{1,2}

¹Centro de Investigación Príncipe Felipe, Valencia, Spain

²Servicio de Neurocirugía. Instituto de Neurociencias. IdISSC, Hospital Clínico San Carlos, Universidad Complutense de Madrid, Madrid, Spain

³Centro de Biomateriales e Ingeniería Tisular, Universidad Politécnica de Valencia, Valencia, Spain

⁴Networking Research Center on Bioengineering, Biomaterials and Nanomedicine (CIBER-BBN), Zaragoza, Spain

Key Words: biomaterials, polycaprolactone, ensheathing glia, axonal growth, neurodegenerative diseases

Abstract: Repair of central nervous system (CNS) lesions is difficult by the lack of ability of central axons to regrow, and the blocking by the brain astrocytes to axonal entry. We hypothesized that by using bridges made of porous biomaterial and permissive olfactory ensheathing glia (OEG), we could provide a scaffold to permit restoration of white matter tracts. We implanted porous polycaprolactone (PCL) bridges between the substantia nigra and the striatum in rats, both with and without OEG. We compared the number of tyrosine-hydroxylase positive (TH1) fibers crossing the striatal-graft interface, and the astrocytic and microglial reaction around the grafts, between animals grafted with and without OEG. Although TH1 fibers were found inside the grafts made of PCL alone, there was a greater fiber density inside the

graft and at the striatal-graft interface when OEG was cografted. Also, there was less astrocytic and microglial reaction in those animals. These results show that these PCL grafts are able to promote axonal growth along the nigrostriatal pathway, and that cografting of OEG markedly enhances axonal entry inside the grafts, growth within them, and re-entry of axons into the CNS. These results may have implications in the treatment of diseases such as Parkinson's and others associated with lesions of central white matter tracts.

INTRODUCTION

Damage to the central nervous system (CNS), including stroke, trauma and neurodegenerative diseases, constitute the second cause of death and the first cause of disability worldwide. In order to treat these lesions, regenerative medicine has focused in trying to replace the lost neurons. However, the CNS is a very complex structure, where function depends largely on maintaining long distance point to point connections between the different neuronal nuclei through axons contained in the white matter pathways. The CNS is very unpermissive for axonal regeneration. When a lesion occurs, the basal membrane is rapidly reconstituted and a glial scar is formed. Glial cells segregate inhibitory factors¹ which impede axonal growth.²⁻⁵ This may be one of

the causes of the lack of success of cell therapy to treat brain damage. For example, in Parkinson's disease, where dopaminergic cells from the substantia nigra projecting their axons to the striatum are lost, clinical trials have tried to replace the lost dopaminergic cells. Thus, new cells were placed at the striatum, in order to overcome the lack of spontaneous nigrostriatal pathway regeneration. However, the implanted cells were out of control causing the so-called dopaminergic storm, with involuntary movements and other unwanted side effects.⁶

One of the possible solutions for this lack of ability of damaged axons to reestablish long distance connections is to provide of a supporting guide for the axons toward the target structure.⁷⁻¹¹

*These authors contributed equally to this work.

Correspondence to: J. A. Barcia; e-mail: jabarcia@ucm.es

Contract grant sponsor: Regional Government Health Department (Conselleria de Sanitat, Generalitat Valenciana) and Carlos III Health Institute of the Ministry of Health and Consumer Affairs (Spain) (Regenerative Medicine Programme)

Contract grant sponsor: Spanish ministry of Education and Science; contract grant number: MAT 2006-13554-C02-02

Contract grant sponsor: Red de Terapia Celular TERCEL (RETICS), Instituto de Salud Carlos III, Ministerio de Ciencia e Innovación (ISCIII); contract grant number: RD12/0019/0010 (to J.A.)

Contract grant sponsor: Spanish Science & Innovation Ministry; contract grant number: MAT2008-06434 (to M.M.P.)

Contract grant sponsor: "Convenio de Colaboración para la Investigación Básica y Traslacional en Medicina Regenerativa," Instituto Nacional de Salud Carlos III, the Conselleria de Sanidad of the Generalitat Valenciana, and the Foundation Centro de Investigación Príncipe Felipe

Contrary to what happens at the CNS, axons may grow after being severed within the peripheral nerves. Some approaches to overcome the above problem have used bridges made of peripheral nerve grafts into the CNS to enhance central axonal growth.¹²⁻¹⁶ However, issues of availability and histocompatibility of peripheral nerve donors may favor the use of synthetic biomaterials.^{9,10} Among them, polycaprolactone (PCL) is an excellent candidate due to its integrative and biocompatibility characteristics.^{17,18} It can be used to produce macroporous scaffolds, permitting the outgrowth of axons as well as facilitating the arrival of nutrients, and the disposal of metabolic waste.¹⁹⁻²¹ These structures have been used to repair other organs, such as the heart or the urinary bladder.^{22,23}

However, re-entry of axons into the CNS is blocked by the presence of astrocytes and the inhibitory factors referred above. The combined use of cells which have been shown to be permissive to this reentry, such as olfactory ensheathing glial (OEG) cells might overcome this problem.^{16,24-28}

It has been described that cells from the OEG may have a positive effect in degenerative lesions, promoting axonal growth and regeneration, and even remyelination and synaptic reconnection of the damaged axon.^{29,30} This regenerative capacity may be due to the production of trophic factors, like SDF-1 or brain derived neurotrophic factor (BDNF).³¹

In this experiment, we have implanted porous bridges made of PCL, with or without OEG cells embedded inside them, inside the brains of naive rats, between the substantia nigra compacta and the striatum, in order to test the ability of these bridges to convey CNS axonal growth.

MATERIAL AND METHODS

All procedures were performed under the standard criteria for ethical management and care of the animals in accordance with the EC Council Directive of November 24, 1986, and approved by the local ethics committee of the Centro de Investigacion Principe Felipe de Valencia.

OEG isolation and culture

OEG cells were isolated from four adult homozygotic transgenic rats (Wistar-TgN[CAG-GFP]184 years) with constitutive expression of enhanced green fluorescent protein (eGFP) (Rat Resource and Research Center, University of Missouri, according to the procedure described by Navarro et al.³² Briefly, rats were anesthetized with pentobarbital sodium (60 mg/kg, Sigma) and decapitated. The two outer layers of the olfactory bulb were dissected, minced, and then trypsinized with 0.25% trypsin and 0.03% collagen enzyme IV for 15 min at 37°C. After two centrifugations (1000 rpm, 10 min), the pellet was suspended in Dulbecco's Modified Eagle's Medium (DMEM)/F12 (Gibco) with 10% fetal bovine serum (Gibco), 1% glutamine (Hyclone), 2% penicillin-streptomycin (Hyclone), and 1% gentamicin (Hyclone) and seeded into a 60-mm cell culture dish (Corning) with 5×10^6 cells and incubated for 24 h (37°C and 5% CO₂). Cells in passage 4 were prepared to be implanted following the method proposed by the laboratory of Gómez-Pinedo et al.³³

Polymeric materials

PCL (molecular weight (MW): 48,000, density 1.145 g/cm³; Polysciences) was employed to develop the porous materials. Poly(ethyl methacrylate) (PEMA) beads (Elvacite 2043; DuPont), having a size of around 200 ± 25 μm, were used as the porogen material. Besides, ethanol (EtOH) (99.5%; Scharlau) and 1,4-dioxane (98% purity, Scharlab) were used in the scaffold fabrication procedure. Each of these materials was employed as received.

Fabrication of scaffolds

A solution of 10% (w/w) of PCL in 1,4-dioxane was mixed with an appropriate quantity of acrylic microspheres in a teflon mold and frozen using liquid nitrogen. The extraction of the frozen mold was carried out in cold ethanol at 220°C (ethanol was changed three times over 3 days) and then porogen was leached using ethanol at 40°C in a shaking bath. Ethanol was changed until no more porogen was detected in the washing solution. Then samples were allowed to dry in air during 24 h and further dried in vacuum for 72 h. Samples were cut using a scalpel to dimensions 1.3 × 1.3 × 6 mm and sterilized using γ-ray irradiation at a standard dose of 15 kGy.

Scanning electron microscopy observation

For scaffold morphology characterization, samples were fractured in liquid nitrogen, mounted on copper stubs, and gold sputtered. The samples were observed with a JEOL JSM6300 scanning electron microscope under an acceleration field of 10 kV.

Porosity determination

Porosity was calculated by gravimetric means. Samples were weighed dry, filled with ethanol under vacuum, and subsequently weighed again. Porosity was calculated as the quotient of the volume of pores and the total apparent volume of the scaffold. The volume of pores was calculated as the ratio between the weighed mass of ethanol within the scaffold and ethanol density; the apparent volume occupied by the scaffold was taken as the sum of the pore volume and the polymer volume, and the polymer volume was determined as the ratio of the weighed polymer mass and the density of PCL. Five independent measurements were performed.

The PCL-grafts were stereotactically implanted using a procedure already described.³⁴ Briefly, animals were anesthetized and placed in a stereotaxic instrument permitting trajectories with different entry angles (Stellar, Stereotaxic Instrument 5100, Stoelting Co., IL). Coordinates were determined for the insertion of a graft between the center of the striatum and substantia nigra pars compacta. The coordinates from bregma, according to the Paxinos and Watson³⁴ atlas, were 21.5 mm lateral (X1), 25.6 mm posterior (Y1), and 28.4 mm below the dural surface (Z1) for the substantia nigra pars compacta, and 24.0 mm lateral (X2), 20.8 mm posterior (Y2), and 25.5 mm dorso-ventral (Z2) for the center of the striatum. The graft's length (or distance between substantia nigra and striatum) measured 6 mm and the entry angles were alpha (zenital) 5° 22.28 and beta (azimuthal) 5° 27.58. A specially designed cannula permitted the placement of the

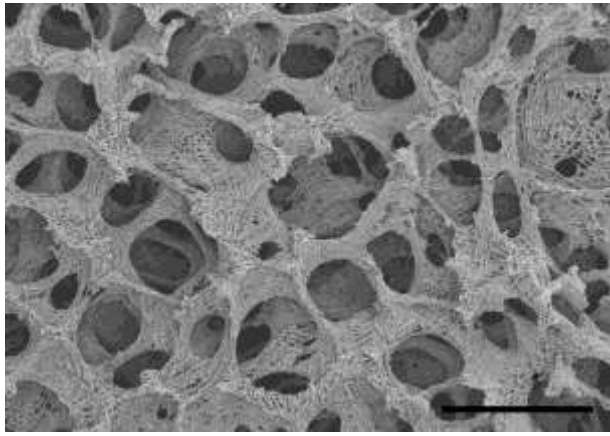


FIGURE 1. Scanning electron image of PCL shows a view of the inner porous structure of the scaffold. It presents a bimodal pore size distribution, with large macropores around 250 μm interconnected and micropores with dimensions ranging from 30 to $<5 \mu\text{m}$. Porosity of the scaffold as measured by gravimetric means was $90.5 \pm 1.7\%$. Scale bar: 300 μm .

PCL-grafts between the two targets without pushing or squeezing them, with a piston preventing the graft from sliding back. In the experimental group ($n = 8$) we injected at the distal and proximal end of the PCL-grafts 2 mL of a suspension of OEG cells (5.3×10^4 cells), while in the control group ($n = 8$) the PCL-grafts was implanted without further manipulation. Although the host animals had not been previously manipulated before the implant procedure, the insertion of the PCL-grafts could have produced a local mechanical lesion at the implant trajectory.

Four weeks after grafting, animals were sacrificed through barbiturate overdose, perfused with 4% paraformaldehyde (PFA), removed brains postfixed in 4% PFA solution, and embedded in Tissue-Tek. Transverse sections of 20 μm were cut and mounted on slides. An anti-tyrosine hydroxylase (TH) monoclonal antibody (Millipore MAB318; 1:1000) was used to observe the substantia nigra, and the dopaminergic cells and fibers. An anti-glial fibrillary acidic protein (GFAP) polyclonal antibody (DakoCytomation Z0338; 1:300) was used to analyze the glial reaction, for microglial identification, a monoclonal anti-IBA-1 antiserum (Wako; 1:500) and an anti-green fluorescent protein (GFP) polyclonal antibody (ABCAM AB13970; 1:200), was used to label GFP cells, followed by Alexa secondary antibody 488, 555 and 647 anti-mouse or anti-rabbit.

Immunohistochemistry samples were observed in an optical microscope (Leica DM 6000B, Leica Microsystems) or a confocal microscope (Leica SP2, ABOS Leica Microsystems). To obtain confocal micrographs, each fluorochrome dye within the same field was scanned separately.

Fluorescence images were quantified using the software included in the confocal microscope (Leica SP2, ABOS Leica Microsystems). To measure TH fibers, we applied a modification of the physical disector method described by Reed, using the unbiased brick principle of the three-dimensional disector.^{35,36}

In order to evaluate the microglial and glial reaction in the area close to the striatal end of the graft (100 μm around), we used a modified version of Sholl rings.³⁷ Briefly, the

stereological graticule consists of concentric circles with 10 μm of distance between each. The cellular somata with their visible branches were placed on the center of the graticule and the number of intersections (NoI) of radial glial cell-like processes projections within the graticule was counted.

Quantitative results are expressed as mean \pm standard error of mean. Groups were tested for differences by performing *t* student test following a Mann Whitney test using Prism (GraphPad Software Inc., La Jolla, CA). Differences were considered statistically significant at a value $p < 0.05$.

RESULT

The biomaterial produced presented the structure of a scaffold with a high porosity. This can be shown in Figure 1, where pores of 300 μm are shown beside 5 to 30 μm micropores contributing to connect between them, permitting the passing through of cells and fluids.

All animals survived after the grafting procedure. There were no behavioral or neurologic deficits, and no seizures were observed. The brains showed no macroscopic signs of inflammation, infection or rejection of the biomaterial. Histological analysis with serial sections demonstrated that the graft was correctly placed between the two points chosen and integrated with the host brain. An astrocytic reaction was evident around the graft, without cavitations, edematous or necrotic areas, neutrophil infiltrates or other histologic alterations suggesting rejection. This astroglial reaction was more evident in the grafts implanted without OEG cells, which were encapsulated by the scar and showed protoplasmic astrocytes. When OEG had been cografted, only a mild astroglial reaction was observed, and the morphology of most of the astrocytes was similar to the intact areas of the brain located far from the implant: non-hypertrophic stellate astrocytes with fine filaments. The quantitative analysis of the astrocytic transformation in terms of number of GFAP marked cells per 500 μm^2 reflects this difference (Figure 2, $p < 0.05$). Figure 2 approximately here.

Also, a discrete microglial reaction in the vicinity of the implanted biomaterial was observed. When OEG was cografted

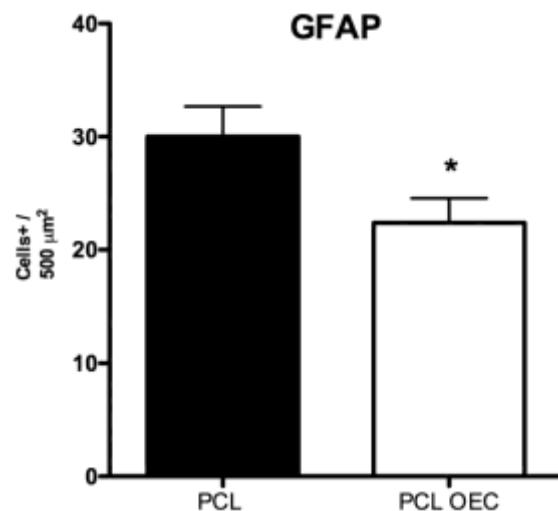


FIGURE 2. Mean density of GFAP marked cells around the implant in both groups. * $p < 0.05$.

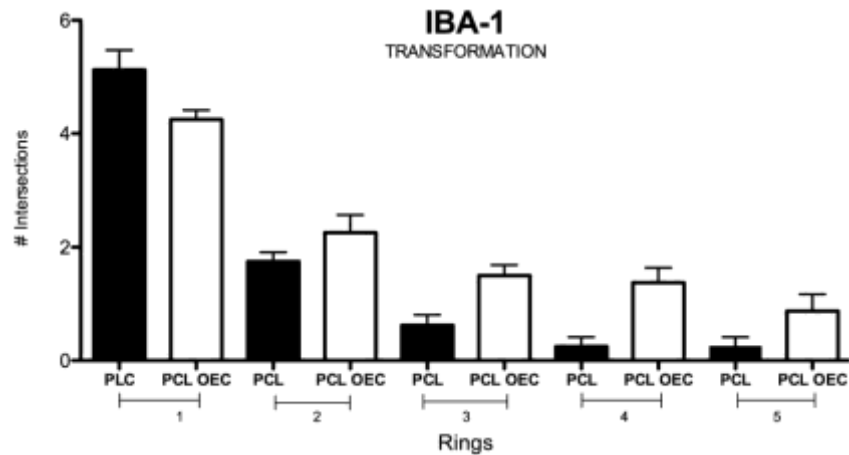


FIGURE 3. Quantification of the microglial transformation around the biomaterial, showing the expression of IBA-1 within concentric rings with 10 μ m of distance between each. Expression greater within the innermost rings indicates more amoeboid shape, and expression within the outermost, a more branching shape. Microglial cells in resting state tend to be more branching.

the morphology of microglia was similar to other normal brain areas (quiescent microglial cells), while grafts without OEG were surrounded by amoeboid rod-shaped microglial cells forming a small layer around the graft. (Figure 3, $p < 0.05$).

TH1 fibers were seen inside the grafts (in both cases) (Figures 4 and 5), although the fiber density was higher when OEG was cogenerated (Figures 5 and 6). OEGs were

even seen migrating inside the grafts. Fiber count inside the graft showed a higher density at the substantia nigra end, and a progressive reduction of fiber density in the middle and in the striatal end of the graft (Table I, $p < 0.05$).

DISCUSSION

Results show that bridges made of PCL support the growth of axons to connect two distant nuclei within the CNS.

Up to now, the only way to produce this was inserting biologically derived materials, either endogenous or allogenic. Peripheral nerve grafts have been widely used due to their capacity to sustain axonal growth. Also, injection of biochemicals to inhibit astrocytic activity and create a local milieu permissive to axonal growth. Collier and Springer³⁷ were able, using peripheral nerve grafts with embryonic dopaminergic cells in hemiparkinsonian rats, to recover the neurotransmitter levels improving the motor activity of the damaged rats.³⁸ Wictorin et al. were able to show axons reaching the striatum through Schwann cell grafts in 6OHDA damaged rats, without an effect on motor behavior.³⁹ The transplantation of fetal dopaminergic neuroblasts in damaged animals may generate a histological pattern resembling the nigrostriatal pathway suggesting a functional integration.

However, up to now no one has demonstrated that the anatomical reconstruction is superior to simply grafting the striatum with dopaminergic neurons. One of the reasons for this may be the limited number of axons reaching their final target. The use of polymeric biomaterials oriented in longitudinal fascicles may be a means to obtain a richer axonal regrowth.

The grafting procedure is original (previously reported in Gómez-Pinedo et al.)³³ and was designed to implant peripheral nerve grafts. It was designed to overcome the difficulty of placing a flaccid material joining two desired nuclei within the CNS. It has been useful to implant biomaterials with the consistency of PCL, the grafts being placed connecting the desired CNS nuclei. The procedure did not produce any observable side effects, in terms of general or neurological behavior, inflammation, infection or rejection.

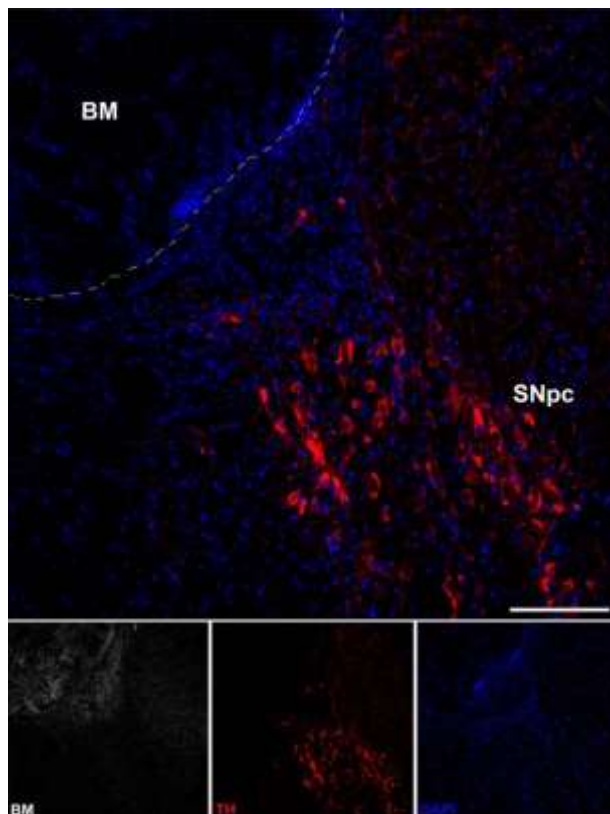


FIGURE 4. Confocal microscopic picture of the PCL only implant close to the substantia nigra pars compacta (SNpc), showing a low density of TH fibers within the biomaterial. BM, biomaterial; TH, tyrosine hydroxylase; DAPI, 4',6-diamidino-2-phenylindole. Scale bar: 200 μ m.

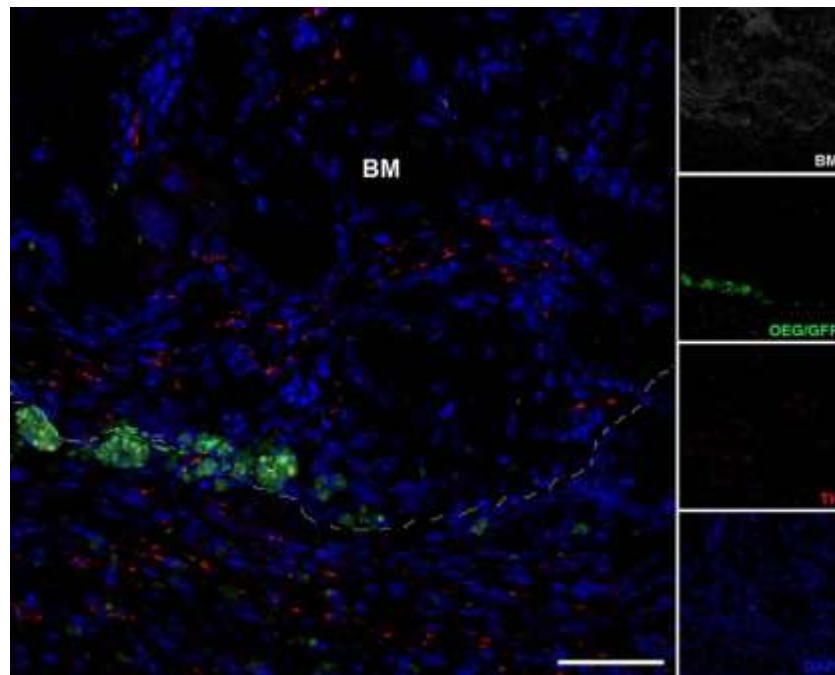


FIGURE 5. Confocal microscopic picture of the PCL plus OEG implant, showing the OEG cells at the border of the biomaterial and a higher TH fiber density within the implant. TH fibers within the biomaterial. GFP, green fluorescent protein; BM, biomaterial; TH, tyrosin hydroxylase; DAPI, *. Scale bar: 75 μ m

Also, the PCL graft has shown to be biocompatible with the brain, integrating with the host tissue, not producing toxic side effects, as already described by other authors,^{19,21,22} thus able to provide a bridge between the two desired points within the brain. Cograftering the OEG cells was associated with a better integration of PCL grafts with the host brain. PCL had already been shown to be permissive to neural growth. *In vitro*, neural cells grow over the surface of 2D films made of PCL and show a normal electrophysiologic activity.^{40,41} PCL has seldom been used *in vivo* in the CNS. Pérez-Garnés et al.⁴² showed that PCL can safely be implanted over the meninges, without an inflammatory response. Other biomaterials have been used more frequently in central neural implants, such as hyaluronic acid, chitosan, or carbon nanotubes.⁹⁻¹¹ However,

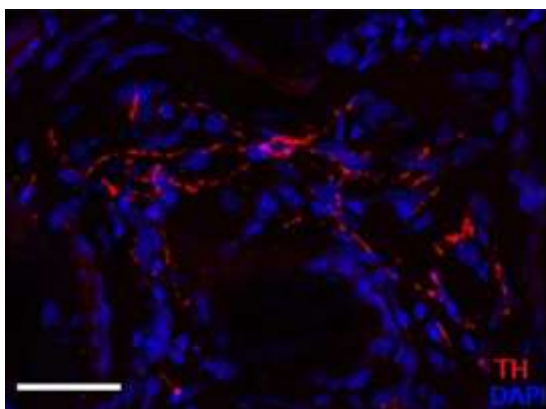


FIGURE 6. Detail of the interior of the PCL plus OEG implant, where TH positive axons are seen within the biomaterial, as well a high density of cells colonizing the implant.

PCL is easily produced, is biocompatible, modulates the microglial and astrocytic response and is permissive for the growth of neurites, although its production is expensive and needs more safety studies in humans. PCL also showed to be compatible to OEG cograftering. The use of OEG and other cells which enhance axonal growth associated to biomaterials has already been tested^{43,44} and could be a proper strategy to adapt the artificial grafts to the repair of brain injuries.

Although there was an astrocytic reaction around the graft, trying to encapsulate the graft, it was mild enough to permit the entry of axons. Also, there was a microglial reaction, indicating a local brain reaction to a foreign body, not important enough to shown signs of graft rejection. Astrocytic and microglial reaction was lower when OEG was cograftered, indicating that OEG promotes a microenvironment with less inflammation, which could constitute the mechanism of its enhancing effect on axonal regeneration.

Axons positive to TH1 (i.e., axons from dopaminergic cells) were seen inside the grafts both when PCL was implanted alone and when OEG was cograftered. As TH1 fibers have been seen crossing the graft interface at both ends of the grafts, and

TABLE I. Mean Number of TH Fibers Within the PCL Implant in Both Groups^a

Number of TH1 Fibers		
Zone	PCL	PCL-OECs
SN interface-graft	106 6 8.2	133 6 11.1
MW	57 6 4.8	72 6 9.9
ST interface-graft	39 6 4.1	62 6 3.4

^a Volume analyzed (0.077 mm³).

dopaminergic fibers grow only from the SN part of it, it is possible to conclude that the fibers enter the graft at the nigral end, and also that they exit the graft at the striatal end.

This is supported by the fact that fiber density is highest at the nigral end and progressively lower along the direction toward the striatal end. Cograftering of cells permissive to fiber reentry into the CNS, such as OEG, markedly increases this effect, being even more marked at the striatal end, that is, it enhances axonal entry inside the graft, growth within the graft and specially reentry of axons back into the CNS. OEGs were seen migrating inside the grafts. The fact that OEG cells have been found along the graft and not only at the extremes, where they were injected, may support the idea that these cells migrate inside the graft and enhance the axonal growth along the graft. They also greatly enhance the reentry of axons inside the brain.

OEGs permit the entry of axons from the olfactory nerves into the olfactory bulb^{24-26,45} and have been extensively used as permissive cells for axonal reentry in spinal cord and spinal root repair.^{27,33} In our study, OEGs have favored the entry of dopaminergic axons into the graft and they have also permitted the reentry of axons back into the brain.

We chose implanting our grafts close to the substantia nigra pars compacta due to the specific ability of dopaminergic fibers to regrow.^{16,46}

This study is limited because we have not shown reinnervation of the tissues from axons coming from the graft. Also, it has to be followed by studies showing histological and functional reinnervation in animal models of axonal injury or neurodegeneration, such as models of parkinsonism, in order to demonstrate the potentially clinical usefulness of this strategy.

ACKNOWLEDGMENT

We are grateful to the Confocal Microscopy Service at the Centro de Investigación Príncipe Felipe (Valencia, Spain).

REFERENCES

- Pekny M, Wilhelmsson U, Pekna M. The dual role of astrocyte activation and reactive gliosis. *Neurosci Lett* 2014;565:30–38
- Bliss TM, Andres RH, Steinberg GK. Optimizing the success of cell transplantation therapy for stroke. *Neurobiol Dis* 2010;37:275–283.
- Tam RY, Fuehrmann T, Mitrousis N, Shoichet MS. Regenerative therapies for central nervous system diseases: A biomaterials approach. *Neuropsychopharmacology* 2014;39:169–188.
- Skop NB, Calderon F, Cho CH, Gandhi CD, Levison SW. Improvements in biomaterial matrices for neural precursor cell transplantation. *Mol Cell Ther* 2014;2:19.
- Yasuhara T, Kameda M, Sasaki T, Tajiri N, Date I. Cell therapy for parkinson's disease. *Cell Transplant*. 2017;26(9):1551–1559.
- Orive G, Anitua E, Pedraz JL, Emerich DF. Biomaterials for promoting brain protection, repair and regeneration. *Nat Rev Neurosci* 2009;10:682–692.
- Walker PA, Aroom KR, Jimenez F, Shah SK, Harting MT, Gill BS, Cox CS. Advances in progenitor cell therapy using scaffolding. *Constructs for central nervous system injury. Stem Cell Rev* 2009; 5(3):283–300.
- Zhong Y, Bellamkonda RV. Biomaterials for the central nervous system. *J R Soc Interface* 2008;5:957–975.
- Meng F, Modò M, Badyalak SF. Biologic scaffold for CNS repair. *Regen Med* 2014;9:367–383.
- Pérez-Garnez M, Barcia JA, Gómez-Pinedo U, Monleón-Pradas M, Vallés-Lluch A. Materials for Central Nervous System Tissue Engineering. *Cells and Biomaterials in Regenerative Medicine. InTech*; 2014. Chap 7.
- Tello F. La regeneración de las vías ópticas. *Trab Lab Invest Biol* 1907;5:237–248.
- Tello F. La influencia de la neurotropismo en la regeneración de los centros nerviosos. *Trab Lab Invest Biol* 1911;9:123–159.
- Vidal-Sanz M, Bray GM, Villegas-Pérez MP, Thanos S, Aguayo AJ. Axonal regeneration and synapse formation in the superior colliculus by retinal ganglion cells in the adult rat. *J Neurosci* 1987; 7(9):2894–2909.
- Benfey M, Bünger UR, Vidal-Sanz M, Bray GM, Aguayo AJ. Axonal regeneration from GABAergic neurons in the adult rat thalamus. *J Neurocytol* 1985;14(2):279–296.
- Gómez-Pinedo U, Videira S, Sancho FJ, García-Verdugo JM, Matías-Guiu J, Barcia JA. Olfactory ensheathing glia enhances reentry of axons into the brain from peripheral nerve grafts bridging the substantia nigra with the striatum. *Neurosci Lett* 2011;494(2):104–108.
- Sinha VR, Bansal K, Kaushik R, Kumria R, Trehan A. Poly-epsilon-caprolactone microspheres and nanospheres: An overview. *Int J Pharm* 2004;278:1–23.
- Mas Estelles J, Vidaurre A, Meseguer Duenas JM, Cortazar IC. Physical characterization of poly-caprolactone scaffolds. *J Mater Sci Mater Med* 2008;19:189–195.
- Sun H, Mei L, Song C, Cui X, Wang P. The in vivo degradation, absorption and excretion of PCL-based implant. *Biomaterials* 2006;27:1735–1740.
- Hollister SJ. Porous scaffold design for tissue engineering. *Nat Matters* 2005;4:518–524.
- Izquierdo R, Garcia-Giralt N, Rodriguez MT, Cáceres E, García SJ, Gómez Ribelles JL, Monleón M, Monllau JC, Suay J. Biodegradable PCL scaffolds with an interconnected spherical pore network for tissue engineering. *J Biomed Mater Res A* 2008;85(1):25–35.
- Lee JN, Chun SY, Lee HJ, Jang YJ, Choi SH, Kim DH, Oh SH, Song PH, Lee JH, Kim JK, Kwon TG. Human urine-derived stem cells seeded surface modified composite scaffold grafts for bladder reconstruction in a rat model. *J Korean Med Sci* 2015;30:1754–1763.
- Wan L, Chen Y, Wang Z, Wang W, Schmill S, Dong J, Xue S, Imboden H, Li J. Human heart valve-derived scaffold improves cardiac repair in a murine model of myocardial infarction. *Sci Rep* 2017;4(7):39988.
- Raisman G. Olfactory ensheathing cells—another miracle cure for spinal cord injury? *Nat Rev Neurosci* 2001;2(5):369–375.
- Raisman G, Li Y. Repair of neural pathways by olfactory ensheathing cells. *Nat Rev Neurosci* 2007;8(4):312–319.
- Fairless R, Barnett SC. Olfactory ensheathing cells: Their role in central nervous system repair. *Int J Biochem Cell Biol* 2005;37(4): 693–699.
- Yazdani SO, Pedram M, Hafizi M, Kabiri M, Soleimani M, Dehghan MM, Jahanzad I, Gheisari Y, Hashemi SM. A comparison between neurally induced bone marrow derived mesenchymal stem cells and olfactory ensheathing glial cells to repair spinal cord injuries in rat. *Tissue Cell* 2012;44(4):205–213.
- Chou H, Lu CY, Wei-Lee, Fan JR, Yu YL, Shyu WC. The potential therapeutic applications of olfactory ensheathing cells in regenerative medicine. *Cell Transplant* 2014;23(4–5):567–571.
- Dombrowski MA, Sasaki M, Lankford KL, Kocsis JD, Radtke C. Myelination and nodal formation of regenerated peripheral nerve fibers following transplantation of acutely prepared olfactory ensheathing cells. *Brain Res* 2006;1125(1):1–8.
- Collins A, Li D, McMahon SB, Raisman G, Li Y. Transplantation of cultured olfactory bulb cells prevents abnormal sensory responses during recovery from dorsal root avulsion in the rat. *Cell Transplant* 2017;26(5):913–924.
- Shyu W-C, Liu DD, Lin S-Z, Li W-W, Su C-Y, Chang Y-C, Wang H-J, Wang H-W, Tsai C-H, Li H. Implantation of olfactory ensheathing cells promotes neuroplasticity in murine models of stroke. *J Clin Invest* 2008;118(7):2482–2495.
- Wang B, Li X, Zheng F, Liu R, Quan J, Liang H, Guo S, Guo G, Zhang J. pEGFP-T, a novel T-vector for the direct, unidirectional cloning and analysis of PCR-amplified promoters. *Biotechnol Lett* 2007;29(2):309–312.
- Navarro X, Valero A, Gudiño G, Forés J, Rodríguez FJ, Verdú E, Pascual R, Cuadras J, Nieto-Sampedro M. Ensheathing glia

- transplants promote dorsal root regeneration and spinal reflex restitution after multiple lumbar rhizotomy. *Ann Neurol* 1999;45(2):207–215.
33. Gómez-Pinedo U, Féliz MC, Sancho-Bielsa FJ, Vidueira S, Cabanes C, Soriano M, García-Verdugo JM, Barcia JA. Improved technique for stereotactic placement of nerve grafts between two locations inside the rat brain. *J Neurosci Methods* 2008;174(2):194–201.
 34. Paxinos G, Watson C. *The Rat Brain in Stereotaxic Coordinates*, 4th ed. New York: Elsevier; 2004.
 35. Howard CV, Reed MG. *Unbiased Stereology: Three-Dimensional Measurement in Microscopy*. Oxford: Bioimaging Group; 1998.
 36. Rodrigo R, Cauli O, Gomez-Pinedo U, Agusti A, Hernandez-Rabaza V, Garcia-Verdugo J-M, Felipe V. Hyperammonemia induces neuroinflammation that contributes to cognitive impairment in rats with hepatic encephalopathy. *Gastroenterology* 2010;139(2):675–684.
 37. Collier TJ, Springer JE. Co-grafts of embryonic dopamine neurons and adult sciatic nerve into the denervated striatum enhance behavioral and morphological recovery in rats. *Exp Neurol* 1991; 114(3):343–350.
 38. Timmer M, Müller-Ostermeyer F, Kloth V, Winkler C, Grothe C, Nikkhah G. Enhanced survival, reinnervation, and functional recovery of intrastriatal dopamine grafts co-transplanted with Schwann cells overexpressing high molecular weight FGF-2 isoforms. *Exp Neurol* 2004;187(1):118–136.
 39. Victorin K, Brundin P, Sauer H, Lindvall O, Björklund A. Long distance directed axonal growth from human dopaminergic mesencephalic neuroblasts implanted along the nigrostriatal pathway in 6-hydroxydopamine lesioned adult rats. *J Comp Neurol* 1992;323(4):475–494.
 40. Bourke JL, Coleman HA, Pham V, Forsythe JS, Parkington HC. Neuronal electrophysiological function and control of neurite out-growth on electrospun polymer nanofibers are cell type dependent. *Tissue Eng Part A* 2014;20(5–6):1089–1095.
 41. Nga VDW, Lim J, Choy DKS, Nyein MA, Lu J, Chou N, Yeo TT, Teoh S-H. Effects of polycaprolactone-based scaffolds on the blood-brain barrier and cerebral inflammation. *Tissue Eng Part A* 2015;21(3–4):647–653.
 42. Pérez-Garnés M, Martínez-Ramos C, Barcia JA, Escobar Ivirico JL, Gómez-Pinedo U, Vallés-Lluch A, Monleón Pradas M. One-dimensional migration of olfactory ensheathing cells on synthetic materials: Experimental and numerical characterization. *Cell Biochem Biophys* 2013;65(1):21–36.
 43. Vilarino-Feltre G, Martínez-Ramos C, Monleón-de-la-Fuente A, Vallés-Lluch A, Moratal D, Barcia Albacar JA, Monleón Pradas M. Schwann-cell cylinders grown inside hyaluronic-acid tubular scaffolds with gradient porosity. *Acta Biomater* 2016;30:199–211.
 44. Xie J, Huo S, Li Y, Dai J, Xu H, Yin ZQ. Olfactory ensheathing cells inhibit gliosis in retinal degeneration by down-regulation of the Müller cell Notch signaling pathway. *Cell Transplant* 2017; 26(6):967–982.
 45. Diban N, Ramos-Vivas J, Remuzgo-Martinez S, Ortiz I, Urtiaga A. Poly(L-caprolactone) films with favourable properties for neural cell growth. *Curr Top Med Chem* 2014;14(23):2743–2749.
 46. Zurita M, Otero L, Aguayo C, Bonilla C, Ferreira E, Parajón A, Vaquero J. Cell therapy for spinal cord repair: Optimization of biologic scaffolds for survival and neural differentiation of human bone marrow stromal cells. *Cytotherapy* 2010;12(4):522–537.